Determination of the Crystalline Phases of Poly(vinylidene fluoride) Under Different Preparation Conditions Using Differential Scanning Calorimetry and Infrared Spectroscopy

Marcel Benz, William B. Euler

Department of Chemistry, 51 Lower College Road, University of Rhode Island, Kingston, Rhode Island 02881

ABSTRACT: A method with good precision has been developed to quantitatively measure the degree of α-, β-, and γ crystallinity in poly(vinylidene fluoride) (PVDF) by means of infrared spectroscopy. The phase composition of solution-deposited PVDF films was found to be strongly influenced by the presence of hydrophilic residues on the silicon substrate, the relative humidity present at film deposition, the spatial position on the substrate, and the thermal treatment of the deposited film. Films produced on pristine surfaces gave predominantly α-phase PVDF, but when a layer of polar solvent (acetone or methanol) remained on the surface, the films produced were predominantly γ phase. Higher humidity promoted a higher fraction of γ crystallinity in the solution-deposited PVDF films. Solution-cast films had highly variable composition across the substrate, whereas spin-cast films were uniform. High-temperature annealing of PVDF films normally converts the polymer to the γ phase, but annealing the film while still attached to the silicon substrate inhibited this phase transformation. Low-temperature annealing of freestanding films led to a previously unreported thermal event in the DSC, a premelting process that is a kinetic event, assigned to a crystalline relaxation. Higher-temperature annealing gave a double endotherm, assigned to melting of different-sized crystalline domains. © 2003 Wiley Periodicals, Inc. J Appl Polym Sci 89: 1093–1100, 2003

Key words: crystallization; differential scanning calorimetry (DSC); infrared spectroscopy; phase behavior

INTRODUCTION

Poly(vinylidene fluoride) (PVDF) has been extensively studied because it is a ferroelectric polymer.[1–5] PVDF exists in at least three main crystalline modifications, designated as α (Form II), β (Form I), and γ (Form III), and in at least one minor phase, designated as δ (Form II'). The different forms are distinguished by the conformation of the C—C bonds along the chain backbone. The β phase has all its C—C bonds in the *s-trans* conformation (TTTT), the α phase has alternating *s-trans* and *s-gauche* bonds, (TGT$\bar{\text{G}}$), and the γ phase has an *s-gauche* bond every fourth repeat unit (T$_3$GT$_3\bar{\text{G}}$). The δ phase is very similar to the α-crystalline phase, except that every other chain is rotated and thus is electrically active.[6] The as-cast γ phase has an unordered T$_3$GT$_3\bar{\text{G}}$ sequence mixed with long sequences of *s-trans* conformations.[7,8] The α phase and as-cast γ phase are obtained from solution deposition,[9,10] oriented β phase can be produced by stretching a PVDF film,[11] the γ phase with regularly repeating intervals is obtained by annealing near the melting point, and the δ phase is obtained by poling in an electrical field.[12,13]

The fraction of crystallization of each phase is generally determined quantitatively by X-ray diffraction, but this can be challenging for thin films. Using infrared spectroscopy to quantitatively characterize the crystalline phases hase been attempted,[14] but the measurements were quite imprecise. Gregorio et al.[15] measured the degree of α- and β crystallinity, assuming the IR absorption follows Beer's law. The α phase had a characteristic infrared absorption at 766 cm^{-1}, and these investigators assumed that the 840 cm^{-1} absorption was uniquely characteristic of the β phase. Osaki et al.[16] performed similar estimations for the α- and γ-crystalline phase using the 530 and 510 cm^{-1} IR absorption peaks, respectively, as the phase-specific bands. However, neither method considered the similarity of the β- and γ-crystalline forms and the fact[17] that both these crystalline modifications contribute to the IR absorptions of 510 and 840 cm^{-1}. Thus, an objective of this work was to develop an improved quantitative method for the determination of the three main crystalline phases of PVDF by means of infrared spectroscopy.

A second objective of this study was to better understand the role of the preparation conditions on the phase composition of the deposited PVDF. The IR

method developed allowed us to rapidly assess the degree of crystallinity and the amounts of α-, β-, and γ phases in PVDF polymers. PVDF films were solution-deposited, either by simple casting or spin-casting, and thermally annealed. The four types of crystal modifications strongly depend on the solvent evaporation rate, temperature, and polarity of the solvent.[4,17,18] We found that the phase composition of the initially formed films also depended on the gas-phase humidity, the nature of the substrate surface, and the spatial position of the film on the substrate. Thermal annealing of the pristine films caused further changes in the crystallinity. The thermal behavior was monitored using differential scanning calorimetry (DSC), and we found that every annealing temperature resulted in a different bulk composition of the PVDF. The transformation from the α- to the γ-crystalline form through annealing was described by Prest and Luca.[19] Ishida and coworkers[16,20] studied the crystalline transformation associated with the heat treatment and found the development of a double endotherm in the DSC thermogram of PVDF. The dependence of the double endotherm on the heating rate was studied comprehensively by Wunderlich et al.[21–23] We report here on the results our much more detailed examination of the annealing process at different temperatures. We found that the annealing temperature was a critical feature, with major differences observed if the annealing was done above or below a temperature of about 150°C. Our results indicate that the occurrence of the double endotherm is not linked to the α- to γ-form transformation. Finally, a third endotherm was observed in the DSC thermograms from samples annealed at low temperatures.

EXPERIMENTAL

Polymer solutions

All solvents and chemicals were used as received from Aldrich and Fischer. PVDF powder with a molecular weight of 534,000 was obtained from Aldrich (Milwaukee, WI). The polymer was dissolved in a solvent composed of 90% acetone and 10% dimethylformamide (DMF), sonicated in an ultrasonic water bath below 30°C for 20 min, and then thermostated at 30°C or 37°C for another 30 min without sonication. The PVDF concentration was 50 g/L unless otherwise noted. Some polymer solutions were heated above 50°C for complete dissolution, as described earlier.[24]

Film deposition

The polymer thin films were either deposited by casting from solution or spin coating onto highly polished single-crystal silicon wafers. These wafers were RCA-cleaned (rinsed with acetone, methanol, and deionized water and then N_2 dried) prior to use. Spin coating or -casting was done at room temperature, followed by drying of the polymer film at room temperature or in a temperature-controlled oven. The spin coater from Laurell Technologies Corporation (Model WS-400) was programmed for an acceleration rate of 1245 rpm/s, but different maximum angular velocities and spin times were used. To obtain the oriented crystalline form of PVDF, solution-deposited films were stretched at elevated temperatures as described previously.[25]

Film measurement

IR spectroscopy was performed using a Perkin–Elmer Model 1650 FTIR spectrometer at a 2 cm^{-1} resolution. DSC experiments were measured with a TA Instruments DSC-Q100 calorimeter with modulated capability. The same mass ($\pm$0.1 mg) of PVDF sample was used for each DSC measurement when the width of the melting enthalpy peak at half height was compared. Otherwise, the sample weight was about 10 mg of PVDF thin film. The heating rate was 10°C/min for standard DSC and 2°C/min for modulated DSC, with a modulation period of 50 s. The melting heat enthalpy integration was set from 60°C to 175°C. Infrared spectral manipulations such as baseline correction and offset were performed with the computer program Grams/32 AI (version 6.00; Galactic Industries). The elemental analysis was performed with a Perkin–Elmer 5500 Multitechnique Surface Analyzer with ESCA capability.

RESULTS AND DISCUSSION

Quantitative crystallinity measurement using IR spectroscopy

The α phase of PVDF had a unique IR absorption band at 762 cm^{-1} IR that was baseline separated from all other peaks. In contrast, the β- and γ-crystalline phases resembled each other structurally and spectroscopically and made the differentiation more difficult. The β phase had two distinguishable IR absorption bands, at 468 and 1275 cm^{-1}. The 468 cm^{-1} band had a very small absorption coefficient, and quantitative measurements were insensitive. The 1275 cm^{-1} IR absorption, although a shoulder band, was suitable for quantitative calculations because a reproducible baseline correction could be performed simply using a linear background derived from the main peak. The γ-crystalline form had a unique IR band at 1233 cm^{-1}. However, the 1233 cm^{-1} IR band was also a shoulder, qualitatively very helpful but quantitatively not useful because no baseline correction could be performed independent of the other two crystalline phases. Consequently, the γ-crystallinity had to be accomplished
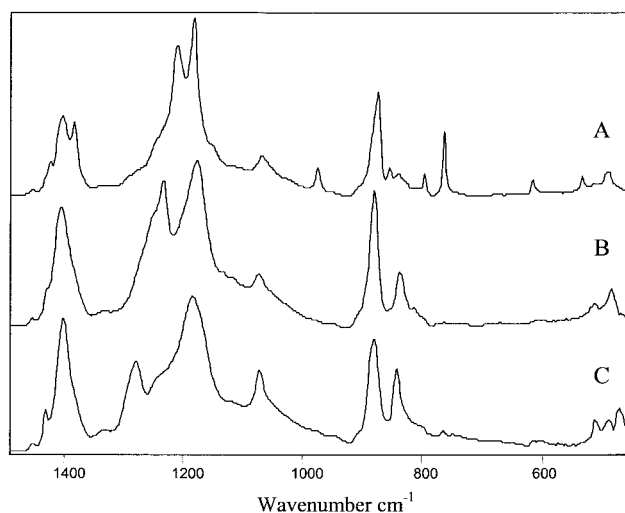
Figure 1 IR spectra of three thin films from the same PVDF solution (dissolved at >50°C): (a) predominant α phase (X_α = 0.46, X_γ = 0.11), film deposited at low humidity (<10%) and on a new wafer; (b) pure γ phase (X_γ = 0.61), film deposited at high humidity (>50%) and on an often-used wafer; (c) predominant β phase (X_α = 0.02, X_β = 0.53, X_γ = 0.08), stretched film (stretching ratio = 3).

with an IR absorption band that accounted for both the β- and γ phases. Two possible IR bands for this purpose were at 510 and 835 cm^{-1}. The 510 cm^{-1} IR band had a much smaller absorption coefficient than did the 835 cm^{-1} band and thus was less sensitive, so we used the 835 cm^{-1} band. To obtain a reproducible baseline for measuring the intensity of the 835 cm^{-1} band, the minima at 860 and 780 cm^{-1} (see Fig. 1) were used as two points on a linear background, which was subtracted from the peak intensity at 835 cm^{-1}. This removed some, but not all, of the intensity resulting from the amorphous phase, so an absorption coefficient for the amorphous was also required.

The crystallinity can be found from the IR spectra using the following equations

$$A_{762} = K_\alpha^{762} X_\alpha t \qquad (1)$$

$$A_{1275} = K_\beta^{1275} X_\beta t \qquad (2)$$

$$A_{835} = (K_\beta^{835} X_\beta + K_\gamma^{835} X_\gamma + K_{am}^{835}(1 - X_{total}))t \qquad (3)$$

where A_j is the baseline-corrected absorbance at j cm^{-1}, K_i^j is the absorption coefficient at j cm^{-1} for the i phase, X_i is the mole fraction of the i phase, X_{total} is the total crystallinity, and t is the thickness in micrometers. The thickness of the PVDF films were determined as described previously[25] using the IR absorbance band at 1070 cm^{-1}, which has an absorption coefficient reasonably independent of the crystalline

phase of the polymer—α, β, or γ (A_{1070} = 0.095t + 0.07).

DSC was used to establish the total crystallinity for each sample. The area under the melting peak was compared with the enthalpy of fusion for a 100% crystalline material, ΔH_∞ (ΔH_∞ for PVDF = 104.6 J/g[20,26]) to give X_{total}. This is a valid technique as long as the stretching ratio is less than 3,[27] which was the case for all samples evaluated in this work. Enthalpy values for pure α- and γ-crystalline PVDF are not known and were assumed to be the same, following the work of Prest and Luca.[19] In addition, we did not see different peak widths for the melting endotherm of samples with different crystalline modifications.

Pure α phase PVDF films were obtained by quenching melts in liquid nitrogen or ice water as previously described.[28] This allowed determination of K_{am}^{835} using eq. (3) to be K_{am}^{835} = 0.0259 μm^{-1} (N = 8 samples, standard deviation, σ, = 0.0027). Solution-deposited films always contained both α- and γ phases, as indicated by the IR peaks at 762 cm^{-1}, 1233 cm^{-1}, and 835 cm^{-1}. Using eqs. (1) and (3) gave K_α^{762} = 0.365 μm^{-1} (N = 32, σ = 0.036) and K_γ^{835} = 0.150 μm^{-1} (N = 32, σ = 0.015). Finally, the values for K_β^{835} and K_β^{1275} were found using stretched polymer films. Films that were predominantly α phase but contained a small amount of γ phase ($X_\gamma \sim 0.10$) were stretched at 120°C–150°C to a stretching ratio of no greater than 3. Under these conditions, the α phase was converted to β phase, but the amount of γ phase was left unchanged, as confirmed by the decrease in the intensity of the peak at 762 cm^{-1}, the growth of the 1275 and 835 cm^{-1} bands, and the unchanged intensity at 1233 cm^{-1}. X_γ was established prior to stretching using the absorbance at 835 cm^{-1} and X_α found from the intensity at 762 cm^{-1} after stretching. This gave K_β^{1275} = 0.140 μm^{-1} (N = 24, σ = 0.016) and K_β^{835} = 0.132 μm^{-1} (N = 24, σ = 0.021).

Influence of preparation conditions on crystalline-phase behavior

Equipped with an easy, fast, and reliable method to determine the crystallinity of PVDF thin polymer films, we were able to investigate the crystalline composition of PVDF prepared under a wide variety of conditions. The total amount of crystallinity was found in the range of 50%–65% for all PVDF samples (solution-cast, spin-coated, stretched), coincident with the results of Nakagawa and Ishida.[20] The inhibition of a more complete crystallization of the simple PVDF monomer structure was accounted for by the presence of head-to-head structures in the polymer chain. First, we faced the question of controlling the phase of solution-deposited PVDF films. As described elsewhere,[24] the relative humidity present when depositing a polymer solution has a tremendous effect on the
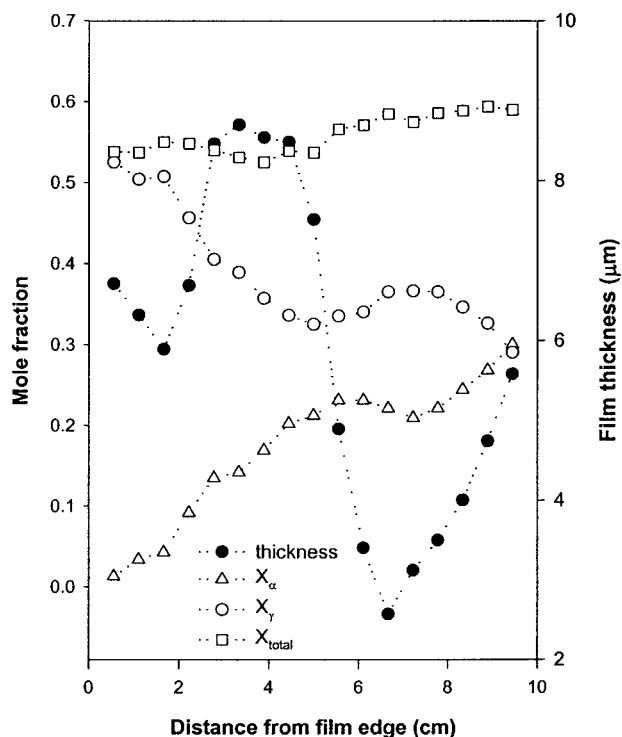
Figure 2 The fraction of crystallinity of (△) α phase, (○) γ phase, (□) total crystallinity, and (●) film thickness along the diameter of a 10-cm-wide solution-deposited PVDF film. The film was cast from an acetone–DMF PVDF solution, dissolved at 30°C, and dried at 50°C. The dotted lines are guides for the eye.

PVDF film surface morphology. Furthermore, we also found that the bulk crystallinity depended on the relative humidity at film deposition. Higher humidity always promoted a higher fraction of γ crystallinity in the PVDF films, presumably because of the electrostatic interactions between water and the polar γ phase. The dissolution temperature of the polymer solution affected the phase composition of the films produced: solutions prepared by dissolving the polymer at high temperatures produced more γ phase. Figure 1 shows the IR spectra of three PVDF films from the same polymer solution. The predominately α- (spectrum A) and γ- (spectrum B) crystalline films were deposited at different relative humidities and on silicon wafers with different histories (*vide infra*). Spectrum C shows a predominately β-crystalline film, obtained by stretching a solution-deposited film. These spectra compare well with the predicted spectra of pure components of PVDF as calculated using principal components analysis.[25]

We also discovered that the crystallinity of solution-cast films could vary enormously within the same film. Figure 2 shows an example of the phase changes across a solution-cast film of about 10 cm in diameter. Although the total crystallinity was relatively constant, the proportions of α- and γ phases changed

substantially across the film. This means that for large area applications, film formation by simple solution casting can lead to variable results. Polymer films that were more uniform in crystallinity and thickness were obtained by spin-coating the polymer solutions. With spin casting the variation in crystallinity and thickness never exceeded 10%.

The second major influence on PVDF phase generation was the substrate. Although the same silicon wafer type was used to deposit the polymer, the number of uses made a difference. The pristine wafers were highly polished single-crystal silicon with about 300 Å of oxide on the surface. Films cast on pristine wafers gave a higher content of the α phase, but used wafers gave increasing amounts of γ phase. ESCA analysis showed an increased carbon content on the used wafers compared to the pristine wafers, but no evidence of fluorine or nitrogen. The residue remaining after use was either acetone or methanol from the previous depositions or RCA cleaning. The residual solvent film of these polar organic molecules induced a higher fraction of the polar γ phase in the deposited PVDF films.

Spin-coated polymer films were dried at different temperatures immediately after deposition. The drying temperature ranged from room temperature to 180°C. The crystallinity of the films was predominately γ phase when dried at less than 80°C and mainly α phase for all films dried at greater than 100°C because of the reduced humidity at higher temperatures. All freestanding films undergo substantial geometrical deformation (shrinking) during annealing. However, dried spin-coated films remained attached to the silicon wafers and so did not undergo significant deformation. Normally, annealing above about 160°C (*vide infra*) induced a transition from α phase to γ phase, but under conditions in which the films remained adhered to the substrate, we found no evidence of an increase in the amount of γ phase. Thus, for the first time we were able to anneal α-crystalline films above 160°C with no transformation to the γ form. Apparently, the surface adhesion was enough to prevent any intramolecular rotation from the TGTḠ to the $T_3GT_3\bar{G}$ conformation.

Annealing and thermal treatment of PVDF strongly influence polymer structure.[29–32] As previously reported,[33] melting points are different for the different crystalline phases of PVDF films. In our measurements, for predominantly α phase, $T_m = 157.9°C \pm 0.6°C$; for pure as-cast γ phase, $T_m = 161.3°C \pm 0.9°C$; and for stretched, predominantly β phase, $T_m = 160°C–161°C$, depending on the film crystallinity before stretching and the stretching rate. All solution-deposited and/or stretched PVDF freestanding films showed only a single melting endotherm in the DSC thermogram. We were interested in the effect on the polymer crystalline phase when a PVDF film was

annealed at successively higher temperatures close to and above the melting temperature. Three polymer films with different crystalline modifications were annealed attached to a metal ring to avoid deformation. The annealing time at increasing temperature was set to 100 h, following the method of Tashiro et al.[34] Figure 3 shows the change in crystallinity of the films, which initially was primarily α phase [Fig. 3(a)], β phase [Fig. 3(b)], or as-cast γ phase [Fig. 3(c)] when annealed at progressively higher temperatures until destruction of the polymer film. In all films the fraction of α phase decreased after its melting point, but annealing above 180°C re-created the α phase (X_γ = 0), although the total crystallinity was reduced. In contrast, the fraction of γ phase increased after an annealing temperature of 160°C until it decreased rapidly after 178°C, which appears to be the melting point of the annealed γ-crystalline phase with a regular repeat sequence. The difference between the as-cast γ phase and the crystalline γ form (annealed) is recognizable in the IR spectrum only as a small split of the 835 cm^{-1} IR band into two bands, at 833 and 839 cm^{-1}. The feature at 833 cm^{-1} was dominant until an annealing temperature of 168°C. Thereafter, it was the 839 cm^{-1} absorption that was more pronounced until the annealed γ phase transformed into the α form at 178°C. In those films with no β phase present initially, there was growth of the β phase when the annealing temperature reached 165°C, but this phase was subsequently destroyed when annealing above 180°C. In the samples in which there was an appreciable fraction of β phase present initially (formed by stretching), there was no increase in the amount of β phase; only loss was observed above 180°C.

The temperature of annealing had a significant impact on the DSC measurements, as shown in Figures 4 and 5. In these experiments all the films initially were predominantly γ phase. At temperatures below the main melting peak, two more enthalpy features (ΔH_1 and ΔH_2) could be found, depending on the annealing temperature, as shown in Figure 4. The lower-temperature enthalpy feature, ΔH_1, appeared only in the samples annealed at temperatures lower than 148°C, and its melting point shifted from 83°C to 153°C with a higher annealing temperature. The higher-temperature enthalpy feature, ΔH_2, appeared only in PVDF films annealed above 135°C, and its melting point shifted from 121°C to 157°C with a higher annealing temperature. As shown in the lower graph in Figure 5, the main melting enthalpy peak, ΔH_m, shifted to higher temperatures with an increased annealing temperature because of the transformation of the as-cast γ phase to the annealed γ phase. The center plot in Figure 5 shows the peak width at half-height for the main melting as a function of annealing temperature. There was a distinct transition in peak width at 148°C, coincident with the loss of ΔH_1 and with the rise in the
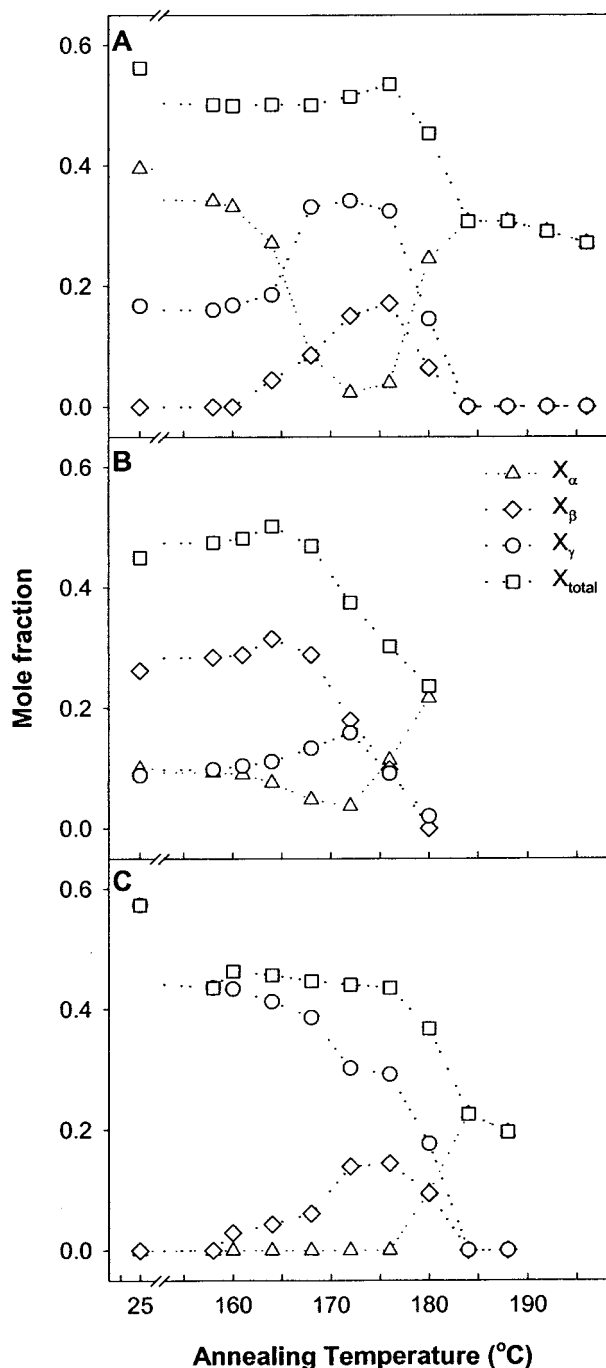

Figure 3 (a) A predominately α-crystalline PVDF film, (b) a predominately β-crystalline PVDF film, and (c) a pure γ-crystalline PVDF film annealed at successively increasing temperatures close to and above the melting point; ($\triangle$) α-crystalline mole fraction phase; ($\diamond$) β-crystalline mole fraction; ($\bigcirc$) γ-crystalline mole fraction; ($\square$) total crystallinity. The dotted lines are guides for the eye.

main melting point. Finally, the top graph in Figure 5 shows the enthalpy for each process. Total enthalpy showed a slight decrease for annealing temperatures above 140°C, consistent with the crystallinity changes noted above. More dramatic changes can be seen with
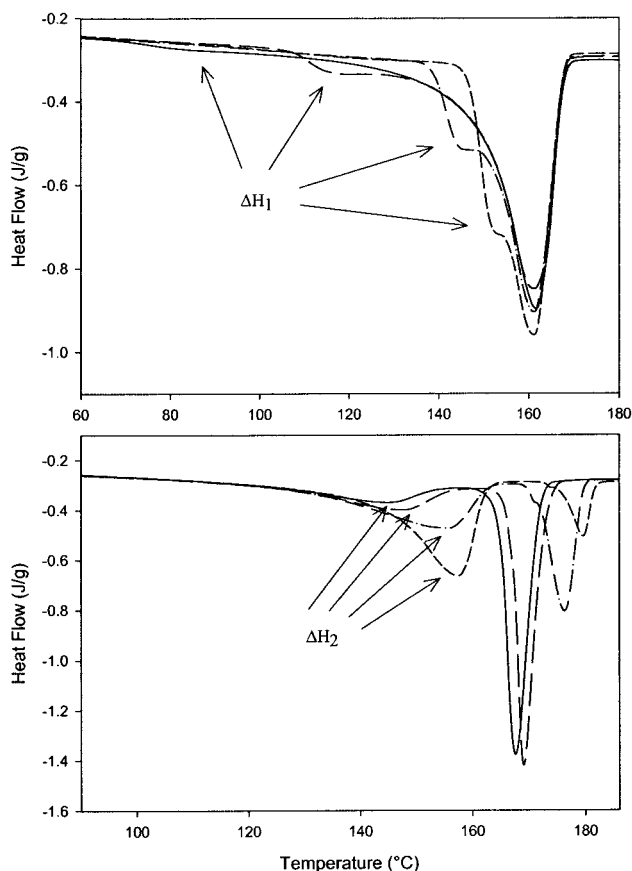
Figure 4 DSC thermograms of annealed PVDF samples. (a) Shift of ΔH_1 toward higher melting temperature: (⌐) annealing temperature of 25°C; (– –) 100°C; (– ·) 135°C; (-) 142°C. (b) Shift of ΔH_2 toward higher melting temperature: (⌐) annealing temperature of 160°C; (–) 163°C; (– ·) 166°C; (—) 169°C.

ΔH_m and ΔH_2. As the annealing temperature was increased, ΔH_m decreased and ΔH_2 increased at 165°C. Finally, the enthalpy associated with the low-temperature feature, ΔH_1, was small for low annealing temperatures, rose slightly for annealing temperatures up to 140°C, and then dropped back to zero.

We performed modulated DSC (MDSC)[35,36] to aid in our interpretation of the nature of the two unassigned enthalpy features, ΔH_1 and ΔH_2. We found that ΔH_1, which occurs in PVDF films when annealed below 148°C, was associated with the nonreversing portion of the MDSC, implying that the heat change is part of a kinetic process. The second enthalpy feature, ΔH_2, which appears in PVDF films when annealed above 135°C, was found in the reversing portion of the MDSC, which is generally thought to signal a thermodynamically reversible process. The integrated area at ΔH_1 was determined for several polymer films annealed at 135°C for different lengths of time. ΔH_1 fit well to a first-order rate expression, $\Delta H_1 = a_0 (1 - e^{-k_{obs}t})$, with $a_0 = 2.72$ J/g and $k_{obs} = 0.099$ min^{-1}. This corresponds to a half-life of only 7 min, a relatively fast process for a polymer.

To determine the required time for the annealing process, freestanding PVDF films (predominately γ phase) were heated at 157°C for different times, ranging from 2 min to 250 h. The results showed that the
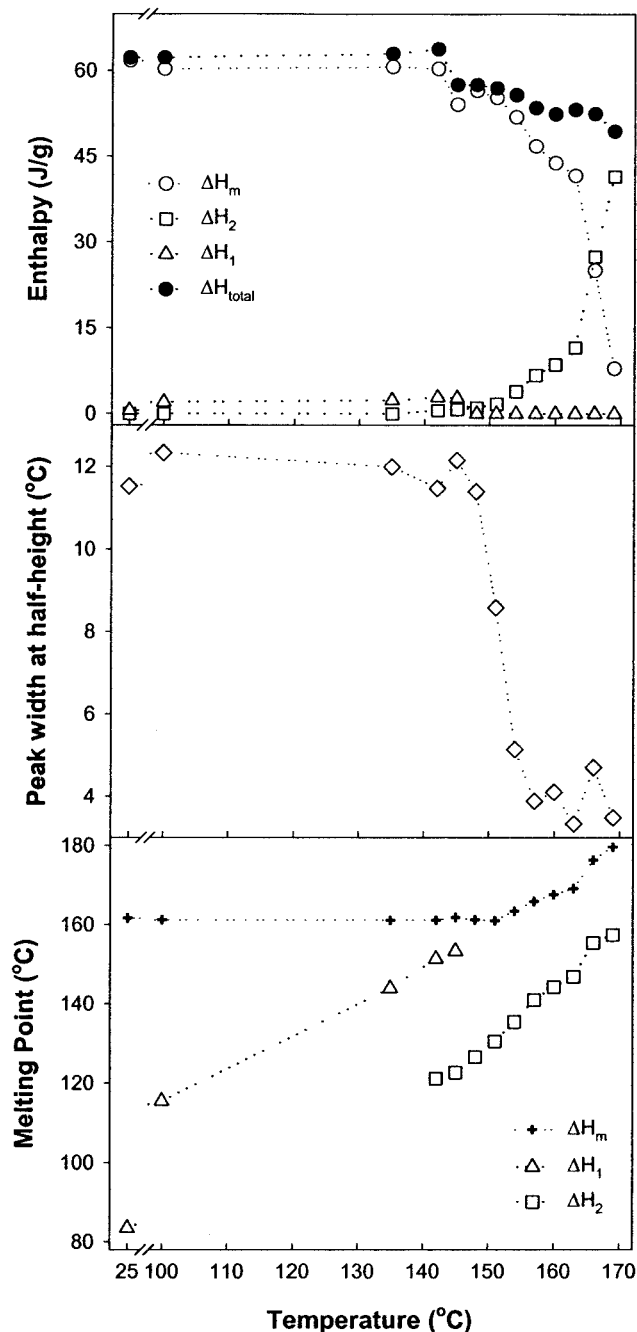

Figure 5 Predominately γ-phase crystalline, freestanding PVDF samples (dissolved at >50°C) annealed at different temperatures and analyzed with DSC. Top graph shows enthalpy versus annealing temperatures: (○) ΔH_m, (△) ΔH_1, (□) ΔH_2, (●) ΔH_{total}. The middle graph plots the melting peak width at (◇) half-height, and the lower graph shows the enthalpies' melting points versus annealing temperatures: ΔH_m, (△) ΔH_1, (□) ΔH_2. The dotted lines are drawn as guides for the eye.

enthalpy width at half peak height was reduced from 12°C to 4.7°C in only 30 min. However, an equilibrated melting point shift from 159°C to 165°C did not occur until 50 h of annealing.

Finally, freestanding, predominately α-phase films were annealed at different temperatures. The α-phase film changed toward an increased γ phase when annealed above 158°C, as previously discussed. The DSC thermograms showed the exact same features as when the γ-phase films were annealed. In addition to the main melting peak, low annealing temperatures (between 25°C and 148°C) gave rise to the ΔH_1 feature, and higher annealing temperatures (above 135°C) induced the ΔH_2 endotherm. The peak associated with ΔH_1 shifted from 75°C to 150°C with an increased annealing temperature, whereas the response at ΔH_2 had peak maxima ranging from 120°C to 157.5°C. As the ΔH_2 feature increased at higher annealing temperatures, the main melting endotherm shifted to a higher temperature, became sharper, and was less intense. These features were observed even for films annealed on the silicon substrate, in which the α-phase to γ-phase transition was suppressed. Thus, we can conclude that each of these heat capacity responses is independent of the phase and so cannot be attributed to changes in conformation along a given polymer chain.

We interpret the DSC data as follows. The first premelting enthalpy feature, ΔH_1, is a crystalline relaxation process, perhaps similar to the alpha-relaxation described by Teyssedre et al.[37] Although Teyssedre et al. did not find any temperature dependence of the alpha-relaxation peak, our results clearly show a shift of the nonreversing enthalpy peak with a higher annealing temperature. The second premelting enthalpy response, ΔH_2, is more complicated. This feature is found in both α-phase and γ-phase samples and so is not caused by an on-chain structural change. Further, the peak maximum and area for ΔH_2 increased with annealing temperature, and the DSC peak width also became narrower, similar to the polymer melting peak. Finally, as the total enthalpy associated with ΔH_2 grew, the enthalpy at the main melting, ΔH_m, and the DSC peak width decreased. Several research reports[16,20,23] have speculated about the origin of the two endothermic peaks (ΔH_2 and ΔH_m). Our results show clearly that the two endotherms are phase independent and that ΔH_m shifts to a higher melting temperature with an increased annealing temperature. These conclusions support the findings of Nakagawa and Ishida,[20] who attributed the higher melting peak (ΔH_m) to the melting of larger and well-formed folded-chain crystals reorganized by annealing. The larger line width of the lower-melting peak (ΔH_2) indicates less ideal crystals and is associated with the melting of smaller crystals. Total crystallinity

does not change significantly because the annealing is only a reorganization of different-sized crystals and is not creating or destroying crystallinity in any notable fashion. Finally, this mechanism is phase independent and does not rely on any conformational changes along the polymer backbone.

CONCLUSIONS

We have established a quantitatively reliable method for determining the crystalline phase composition in PVDF thin films using IR spectroscopy. The technique is fast and simple to apply, thereby allowing for a rapid assessment of the amounts of α-, β-, and γ phases in any PVDF thin-film sample. Using this technique, we examined the composition of PVDF thin films when prepared under a variety of solution deposition and thermal conditions. The gas-phase humidity, the polarity of the substrate surface, the spatial position on the substrate, and the time and temperature of thermal treatment all had a significant influence on the phase composition of the PVDF thin films. Thus, with this detailed information we are now able to produce PVDF films of a desired phase composition using a single solvent system. This work has emphasized the important role of interfacial conditions on the development of crystal phases of thin films in PVDF.

In addition, DSC analyses of annealed PVDF films indicated the presence of previously unreported premelting thermal events and the double endotherm generally found in semicrystalline polymers. When annealed at low temperatures, PVDF was found to have a kinetic process associated with crystalline relaxation in a small portion of the sample. Annealing at higher temperatures removed the kinetic process but introduced the double endotherms that were assigned to melting of different-sized crystals.

References

1. Zhao, Z. X.; Bharti, V.; Zhang, Q. M. Appl Phys Lett 1998, 73, 2054.
2. Omote, K.; Ohigashi, H. J Appl Phys 1997, 81, 2760.
3. Chan, H. L.; Zhao, Z.; Kwok, K. W.; Choy, C. L. J Appl Phys 1996, 80, 3982.
4. Kepler, R. G.; Anderson, R. A. J Appl Phys 1978, 49, 4490.
5. Furukawa, T. IEEE Trans Electrical Insulation 1989, 24, 375.
6. Hasegawa, R.; Takashi, Y.; Chatani, Y.; Tadokoro, M. Polym J 1972, 3, 600.
7. Nalwa, N. S., Ed. Ferroelectric Polymers; Marcel Dekker: New York, 1995.
8. Bachmann, M. A.; Grodon, W. L.; Koenig, J. L.; Lando, J. B. J Appl Phys 1979, 50, 6106.
9. Gregorio, R.; Capitao, R. C. J Mater Sci 2000, 35, 299.

10. Miller, R. L.; Raisoni, J. J Polym Sci, Part B: Polym Phys 1976, 14, 2325.

11. Hasegawa, R.; Kobayashi, M.; Tadokoro, H. Polym J 1972, 3, 591.

12. Hsu, S. L.; Lu, F. J.; Waldman, D. A.; Muthukumar, M. Macromolecules 1985, 18, 2583.

13. Southgate, P. D. Appl Phys Lett 1976, 28, 250.

14. Gregorio Jr., R.; Cestari, M. J Polym Sci, Part B: Polym Phys 1994, 32, 859.

15. Gregorio, R.; Souca Nocita, N. C. J Phys D: Appl Phys 1995, 28, 432.

16. Osaki, S.; Ishida, Y. J Polym Sci 1975, 13, 1071.

17. Kobayashi, M.; Tashiro, K.; Tadokoro, H. Macromolecules 1975, 8, 158.

18. Cortili, G.; Zerbi, G. Spectrochim Acta, Part A 1967, 23A, 2216.

19. Prest, W. M.; Luca, D. J. J Appl Phys 1978, 49, 5042.

20. Nakagawa, K.; Ishida, Y. J Polym Sci 1973, 11, 2153.

21. Hellmuth, E.; Wunderlich, B. J Appl Phys 1965, 36, 3039.

22. Jaffe, M.; Wunderlich, B.; Kolloid, Z. Z. Polym 1967, 216, 203.

23. Liberty, F.; Wunderlich, B. J Polym Sci 1968, A-2, 6, 833.

24. Benz, M.; Euler, W. B.; Gregory, O. J. Langmuir 2001, 17, 239.

25. Benz, M.; Euler, W. B.; Gregory, O. J. Macromolecules 2002, 35, 2682.

26. Maccone, P.; Brinati, G.; Arcella, V. Polym Eng Sci 2000, 40, 761.

27. Teyssedre, G.; Bernes, A.; Lacabanne, C. J Polym Sci: Phys Ed 1993, 31, 2027.

28. Hsu, J. C.; Geil, P. H. J Appl Phys 1984, 56, 2404.

29. Mohajira, B. E.; Heymans, N. Polymer 2001, 42, 7017.

30. Tanaka, R.; Tashiroa, K.; Kobayashi, M. Polymer 1999, 40, 3855.

31. Mohajira, B. E.; Heymans, N. Polymer 2001, 42, 5661.

32. Di Lorenzo, M. L.; Silvestrea, C. Polym Sci 1999, 24, 917.

33. Benedetti, E.; Catanorchi, S.; D'Alessio, A.; Moggi, G.; Vergamini, P.; Pracella, M.; Ciardelli, F. Polym Int 1996, 41, 35.

34. Tashiro, K.; Kobayashi, M.; Tadokoro, H. Macromolecules 1981, 14, 1757.

35. Leray, A. G.; Judovits, L. Proceedings of the 25th North American Thermal Analysis Society 1997, 72.

36. Okazaki, I.; Wunderlich, B. Macromolecules 1997, 30, 1758.

37. Teyssedre, G.; Lacabanne, C. Ferroelectrics 1995, 171, 125.